

Experimental infection of tree shrews (*Tupaia belangeri*) with Coxsackie virus A16

Jian-Ping LI, Yun LIAO, Ying ZHANG, Jing-Jing WANG, Li-Chun WANG, Kai FENG, Qi-Han LI*, Long-Ding LIU*

Institute of Medical Biology, Chinese Academy of Medicine Science, Peking Union Medical Colleg, Kunming 650118, China

Abstract: Coxsackie virus A16 (CA16) is commonly recognized as one of the main human pathogens of hand-foot-mouth disease (HFMD). The clinical manifestations of HFMD include vesicles of hand, foot and mouth in young children and severe inflammatory CNS lesions. In this study, experimentally CA16 infected tree shrews (*Tupaia belangeri*) were used to investigate CA16 pathogenesis. The results showed that both the body temperature and the percentages of blood neutrophilic granulocytes / monocytes of CA16 infected tree shrews increased at 4–7 days post infection. Dynamic distributions of CA16 in different tissues and stools were found at different infection stages. Moreover, the pathological changes in CNS and other organs were also observed. These findings indicate that tree shrews can be used as a viable animal model to study CA16 infection.

Keywords: Coxsackie virus A16; Infection; Tree shrew

Hand-foot-mouth disease (HFMD) is a pathogenesis that mainly affects infantile populations. Although most infection cases show only mild symptoms (Mao et al, 2013), there are a small number of individuals suffering from neurological symptoms of encephalitis and severe heart and lung failure (Tan et al, 2014). From the view of the pathogen, HFMD is mainly caused by enterovirus type 71 (EV71) and Coxsackie virus group A type16 (CA16) infection (Yang et al, 2014). Currently, EV71 vaccine has completed phase III clinical trial (Chen et al, 2014; Li et al, 2014; Zhu et al, 2014), whereas a CA16 vaccine is still under development. Due to the lack of systematic analysis on the infection and immunization of CA16 virus, an effective animal model for CA16 infection is urgently necessary. The conventional animal models of CA16 infection, such as mice or rats (Liu et al, 2014), can neither fully reflect the etiological or pathological characteristics of infection and immunization, nor meet the comprehensive assessment requirements of vaccine safety and efficacy. Non-human primate animal models are of special importance in vaccine evaluation, e.g., Zhang et al (2014) used infant rhesus monkeys (*Macaca mulatta*) to explore the efficacy and safety of EV71 vaccine. However, high cost and limited

animal resources has significantly limited its application. Due to a variety of unique characteristics, e.g., small adult body size, short reproductive cycle and life span (Wang et al, 2013), and especially a close affinity to primates, tree shrews (*Tupaia belangeri*) have been widely applied in biomedical research, especially in virology research (Fan et al, 2013). In this study, 2-month-old tree shrews were used to investigate GX18 infection and their potential as an animal model for CA16 infection was assessed.

MATERIALS AND METHODS

Virus and cells

The CA16 virus used in this study was an isolated GX18 strain from an infected child with mild clinical symptoms in Guilin, China, 2012. The GX18 strain was

Received: 11 April 2014; Accepted: 20 May 2014

Foundation items: This work was supported by the National High-Tech R&D Program (2014ZX09102042), the National Natural Science Foundation of China (81373142) and the Natural Science Foundation of Yunnan Province (2012ZA009)

*Corresponding authors, E-mails: imbcams.lq@gmail.com; longdingl@gmail.com

identified as a CA16 B2 sub-genotype virus by RT-PCR. The virus grown in Vero cells (cultured by Institute of Medical Biology) was harvested for freezing at -20°C with a concentration of $10^{6.5}$ cell culture infectious doses (CCID₅₀)/mL. The Vero cells were maintained in 5% MEM containing fetal bovine serum (provided by Institute of Medical Biology) and grown to a confluent monolayer in a T-25 vessel or in 96-well plates for viral isolation and antibody neutralization assays.

Virus titration and neutralization assay

CA16 harvested from cell culture or isolated from different organs and tissues of infected tree shrews were analyzed by a microtitration assay using a standard protocol (Arita *et al.*, 2006). The neutralization test was performed according to the standard protocol (WHO, 1988). A mixture of diluted serum containing anti-CA16 antibodies (provided by Institute of Medical Biology) and the virus at a titer of 500–1 000 CCID₅₀ in 100 μL of PBS (provided by Institute of Medical Biology) was incubated at 37°C for 1 h. The cellular pathogenic effect (CPE) of the virus was examined by inoculating the mixture onto Vero cells grown in 96-well plates. The plaque assay was performed in 6-well plates containing 90% confluent Vero monolayer cells. The cells were inoculated with samples from blood, throat swabs or feces. After 1 h incubation at 37°C , the infection media were aspirated off and each well was then covered with 3 mL of agar overlay medium and incubated for 2 days at 37°C in a CO₂ incubator. At the end of the incubation, the cells were fixed with formaldehyde and stained with 0.1% Crystal Violet as a standard protocol (Hung *et al.*, 2010).

Tree shrews

Fifteen healthy female tree shrews (80 ± 10 g, 2-month-old) were divided into an infection group ($n=12$) and a mock-infection control group ($n=3$). All animal procedures were approved by the Office of Laboratory Animal Management of Yunnan Province, China. Animals were individually caged and fed according to the guidelines of the Committee of Experimental Animals at the Institute of Medical Biology, Chinese Academy of Medical Sciences (CAMS). Individuals were confirmed free of antibodies against CA16 prior to the experiment via neutralization test.

CA16 infection

Our previous study on EV71 infection in rhesus

monkeys showed that virus distributions in blood and other organs can be observed via intravenous and intratracheal inoculation routes (Zhang *et al.*, 2011). Ong *et al.* (2008) found that infections via intravenous route in cynomolgus monkeys (*Macaca fascicularis*) can not yield a similar distribution of the virus.

In this study, 12 tree shrews were infected with CA16 ($10^{4.5}$ CCID₅₀) via the respiratory tract by nasal spraying. The other 3 tree shrews were mock sprayed by saline as uninfected negative controls. The animals were monitored daily, and their body temperatures were measured rectally by a digital stick thermometer (MC-BOMR, Omron Co.) from day 2 post infection (p.i.). In parallel, venous blood samples were taken into EDTA coated capillary tubes daily for routine detections of biological indicators and viral loads (Veterinary Multi-species Hematology System, Hemavet 950FS, Drew Scientific Co.). Pathogenic and histopathological examinations were performed on all the tissues and organs of tree shrews sacrificed by anesthesia at day 4, 7, 10 and 14 p.i..

Viral RNA extraction and quantitative RT-PCR

Viral RNA was extracted from whole blood (100 μL), fresh tissue homogenate (10%, 100 mg) or fecal homogenate (5%, 100 mg) by TRNzol-A⁺, according to manufacturer's protocols (Tiangen, China). The viral RNA was eluted in a final volume of 20 μL . For quantification, a single-tube, real-time Taqman RT-PCR assay was performed using the Taqman 1-step RT-PCR Master Mix in the 7500 Fast Real-time RT-PCR system (Applied Biosystems, Foster City, CA, U.S.). The reaction mixture (20 μL) contained the Taqman Universal PCR master mix, primers (each at 20 $\mu\text{mol/L}$), the FAM/TAMRA labeled probe (10 $\mu\text{mol/L}$) (Takara Co., Ltd. Dalian, China), and RNA (2 μL). The sequences of the CA16-specific primers and probe were as following: forward primer (5'-ACACTCCATTACCTGAGGGT GTA-3'); probe (5'-ATGAGAATCAAACACGTCAG GGCATGGAT-3'); and reverse primer (5'-ACACTCC ATTACCCTGAGGGTGTA-3'). The following protocol was used for all PCR assays: 5 min at 42°C and 10 s at 95°C , followed by 40 cycles at 95°C for 5 s and 60°C for 30 s. The standard reference curve was obtained by the measurement of the serially diluted virus RNA generated by *in vitro* transcription from a DNA construct that contains the Vp1 region. Viral copies were quantified according to *in vitro*-synthesized RNA by spectrophotometry quantification, and the quantity was

expressed as a relative copy number, determined by the equation: $[(\mu\text{g of RNA}/\mu\text{L})/(\text{molecular weight})] \times \text{Avogadro's number} = \text{viral copy number}/\mu\text{L}$.

Histopathological examination and immunohistochemical analysis

The tissue samples from different organs were fixed in 10% formalin in PBS, dehydrated in ethanol gradients and embedded in paraffin before obtaining 4 μm sections for further H-E staining. Histopathological analysis of the tissue sections from each organ was performed under a light microscope. For the immunohistochemical analysis, tissue samples were embedded in an optimal cutting temperature (OCT) compound (Miles Inc., Elkhart, Ind.) and frozen in liquid nitrogen. The frozen tissues were then cut into 4 μm sections, placed on poly-L-lysine-coated glass slides and fixed in 3.7% paraformaldehyde. The endogenous peroxidase activity of the tissues was inhibited by treating with hydrogen peroxide (2.5%). The CA16 antigen was detected by mouse anti-CA16 sera and horseradish peroxidase (HRP)-conjugated anti-

mouse IgG antibodies (Sigma, Deisenhofen, Germany) followed by color development with diaminobenzidine for the detection of the antigen-antibody reaction.

Statistical Analysis

All the data were expressed as the mean of three samples from all experiments (mean \pm SE).

RESULTS

Clinical observations of CA16-infected tree shrews

No typical papules or vesicles on limbs or mouths were found in infected tree shrews, but increased body temperatures p.i. (Figure 1A), as well as increased percentages of neutrophilic granulocytes and monocytes in some animals (Figure 1B, C) from day 5 to 7 p.i. with the decrease of lymphocyte (Figure 1D) were observed. These findings suggest that similar clinical CA16 infection symptoms as humans (Lo et al, 2011), such as fever and inflammatory responses (reflected in blood cell analysis), can be found in tree shrews.

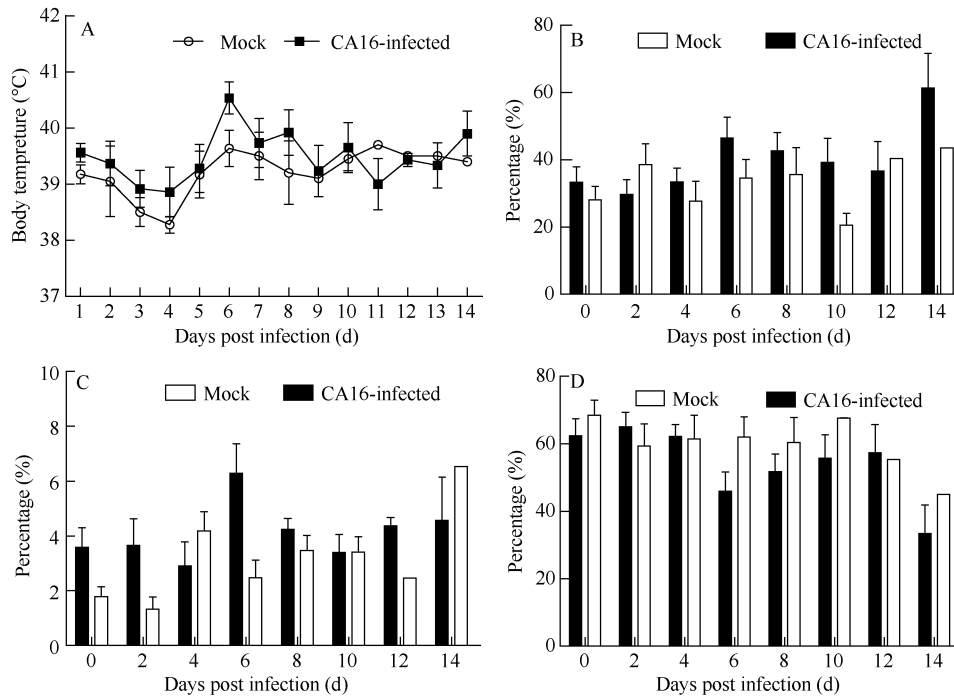


Figure 1 Clinical symptoms of CA16 infected tree shrews via respiratory route

A: Body temperatures of CA16-infected tree shrews; B: The percentage of neutrophilic granulocytes in leukocytes of CA16-infected tree shrews; C: The percentage of monocytes in leukocytes of CA16-infected tree shrews; D: The percentage of lymphocytes in leukocytes of CA16-infected tree shrews.

Dynamic profiles of virus in blood and stool of CA16-infected tree shrews

We analyzed viral load dynamic profiles in blood and stool at different stages of infection. The peak levels

of viral load were observed in the blood (500 copies/100 μL) at day 6 p.i. and in stool (2 000 copies/100 mg) at day 7 p.i., respectively. These findings indicate that the viremia of the infected tree shrews develops from day 3

to day 7 p.i., whereas, the virus shedding in feces is detectable from day 3 to day 14 p.i. (Figure 2B). These virus dynamic profiles imply that the clinical symptoms of CA16-infected tree shrews are correlated with the viremia manifestations.

Viral distributions in tissues from CA16-infected tree shrews

The target organs of CA16 infection in humans involve several different tissues (Wang et al, 2004). To understand the CA16 distributions in tree shrews, the viral loads in various tissues were determined at different stages of infection. CA16 virus was detectable in the lymph node, lung, spleen, kidney, thigh muscle and brain from day 7 p.i.. Relatively high viral loads were found in

the spleen (356 copies/100 mg), cerebellum (290 copies/100 mg), lung (294 copies/ 100 mg), lymph node (200 copies/100 mg), parotid gland (155 copies/100 mg) and thigh muscles (290 copies/ 100 mg), whereas no detectable viral loads were observed in the same tissues of non-infected control tree shrews. In general, viral replication peaked on day 6 or 7 p.i. in the lymph nodes and glands (Figure 3B, C), whereas, peaked on day 10 p.i. in the CNS and spleen, lung and muscles (Figure 3A, D), which might be the major target organs of infection in tree shrews.

It was reported that in certain cases, CA16 is able to target CNS and lead to viral encephalitis (Chang et al, 1999; Goto et al, 2009). In this present study, the total

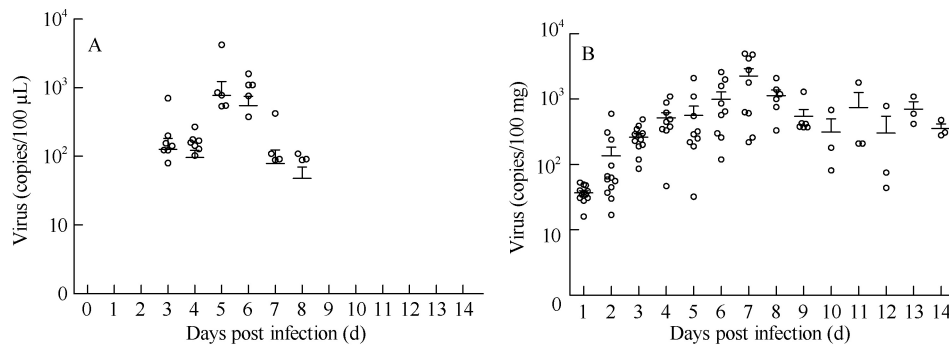


Figure 2 Dynamic distributions of CA16 in the blood and stool of infected tree shrews via respiratory route

A: Viral RNA extracted from blood specimens; B: Viral load in feces.

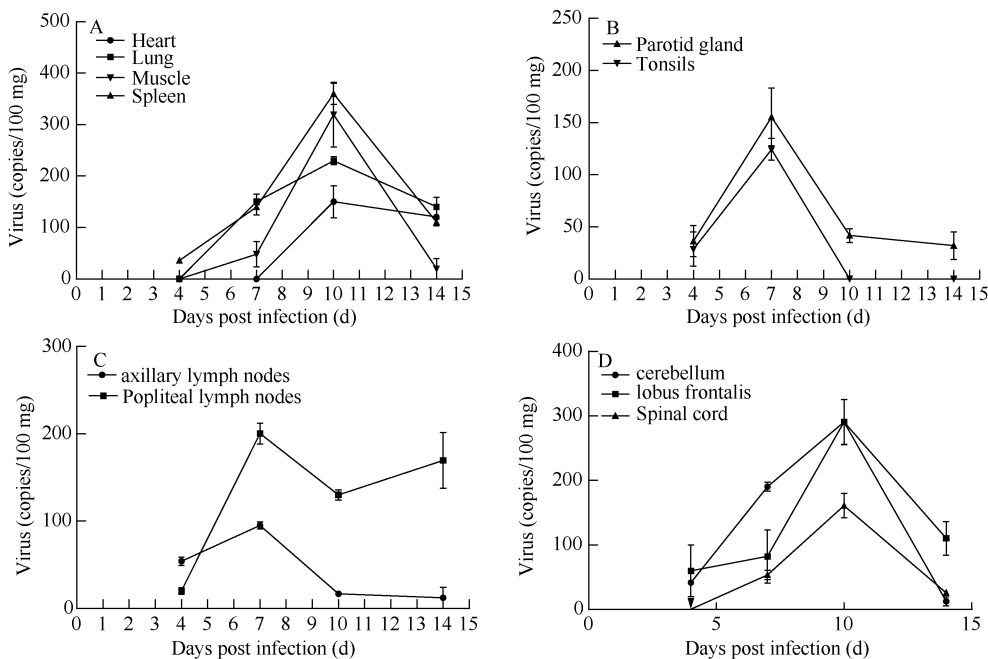


Figure 3 Viral distributions in tissues of CA16-infected tree shrews

A: Viral load in the major organs of infected tree shrews; B: Viral load in glands of infected tree shrews; C: Viral load in the lymph nodes of infected tree shrews; D: Viral load in CNS of infected rhesus monkeys.

distributions of viral loads increased from day 4 to day 10 p.i. (Figure 3B), and higher loads were found specifically in the cerebellum (291 copies/100 mg) and lobus frontalis (294 copies/100 mg) at day 10 p.i., which were consistent with the observation that viral loads peaked in muscles and lungs on day 10 p.i..

Viral antigen detection in tissues from CA16-infected tree shrews

To investigate CA16 replications, antigen expressions of CA16 in the related tissues were examined immunohistochemically. High expressions of viral antigen in the heart (Figure 4A), spleen (Figure 4B) and lung (Figure 4C) were observed. Viral antigens were also observed in the CNS including cerebellum (Figure 4d). These findings are consistent with the patterns of viral load distributions of widespread infections.

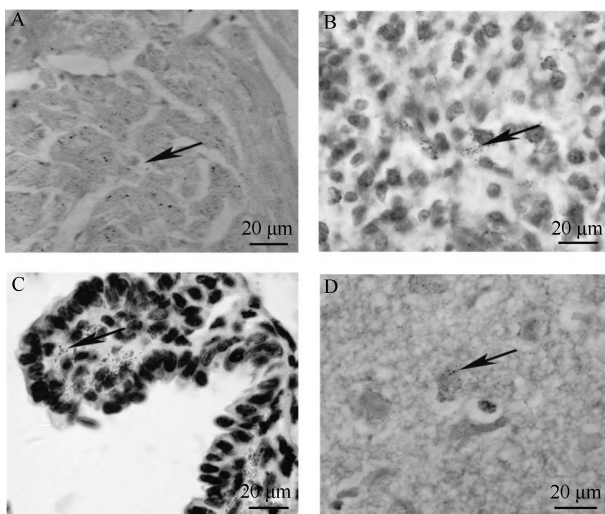


Figure 4 Viral antigen expressions in tissues from CA16 infected tree shrews

A: Sample of the heart collected on day 10 p.i.; B: Sample of the spleen collected on day 10 p.i.; C: Samples of the lung collected on day 10 p.i.; D: Samples of the cerebellum collected on day 10 p.i.; Arrows indicate the stained CA16 antigen; Images are shown at 200× magnification.

Pathological changes in tissues from CA16-infected tree shrews

In this study, the pathogenic changes of CA16 infected tree shrews were evaluated by systematic pathologic analysis on various tissues, including the liver, kidney, spleen, heart, lung, muscles, spinal cord and brain. Pathological responses, such as cell damage and inflammatory cell infiltration (Figure 5A–D) were found in the lung, kidney and muscles, correlating with the presence of high viral loads. The observed neuropathological lesions in the cerebellum indicate that the

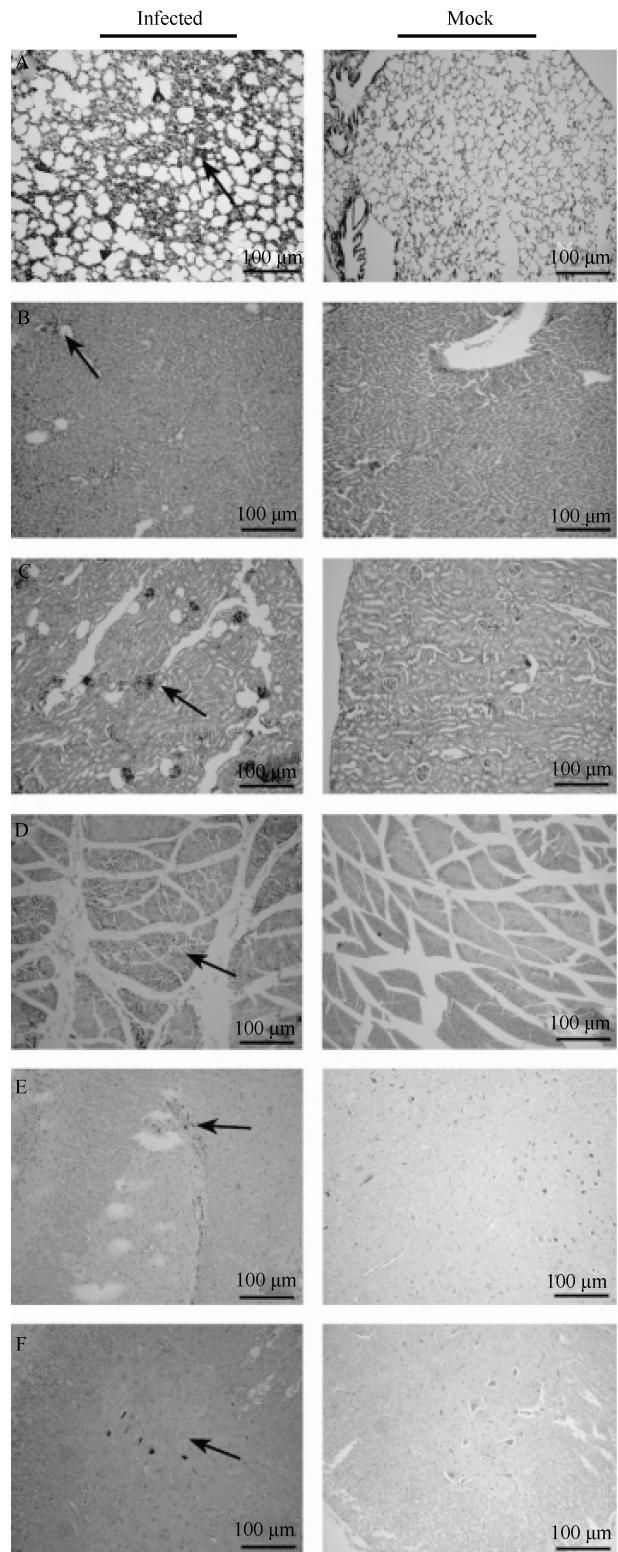


Figure 5 Pathological analyses of CA16-infected tree shrews The typical features of pathological changes as infiltration of inflammatory cells (black arrow) in the lung (A), liver (B), kidney (C) and muscles (D) of CA16 infected tree shrews. Images show the proliferations of neuroglial and neuronal lesions in the thalamus (e) and spinal cord (f) of CA16 infected tree shrews. Images are shown at 200× magnification.

pathogenic changes in CNS may contribute to the degeneration of neural cells, infiltration and inflammatory cell aggregation (Figure 5E, F). Moreover, as expected, all the observed pathological changes were correlated with the viral antigen expressions. These results demonstrate that CA16 has a tropism to the CNS and lung and thereafter may induce severe lesions of these tissues.

DISCUSSION

The establishment of an viable animal model plays critical roles in understanding infectious diseases, such as HFMD, and vaccine evaluations. Animal models of EV71 infection include suckling mice and neonatal rhesus monkeys (Wang et al, 2004; Zhang et al, 2011). The conventional animal model in the studies of CA16 infection is still neonatal mice. The mouse model provides evidence of the protective immunity of CA16 vaccine (Dong et al, 2011) but fails to provide convincing data on the infection pathology and the comprehensive evaluation of vaccine. According to previous reports, tree shrews can be widely used as a potential animal model for many infectious diseases, such as hepatitis C, measles, atypical pneumonia (SARS), tuberculosis, etc (Han et al, 2011; Xu et al, 2013; Yang et al, 2013).

In the present study, experimentally CA16-infected tree shrews have been used to investigate the etiology and pathology of HFMD. In the CA16-infected tree shrews, although no typical vesicles or papules on limbs

and mouth were observed, certain clinical features, such as fever and lymphocyte-related inflammatory responses could mimic some manifestations in human patients with HFMD (Mou et al, 2014; Wang et al, 2013).

The distributions of CA16 virus in tree shrews were determined by viral loads and pathological changes. The high viral loads found in the lymph nodes, heart, lung, spleen, kidney, thigh muscles and brain imply that the respiratory route is one of potential natural infection routes of viral transmissions. The viral load in blood and the antigen expression in the lymph nodes, lung, muscles and CNS indicate that CA16 can spread throughout the whole body of infected animals. Moreover, in this study, high viral loads were detected in cerebellum from day 4 to day 10 p.i., and neuropathological lesions were observed via histopathological examinations. These findings indicate that CA16 infected tree shrews can eventually display a broad range of viral transmission, including CNS. In addition, the viral shedding found in the feces of the infected tree shrews indicate that the typical spreading route of enterovirus can also be demonstrated in this animal model.

Although this study only demonstrates limited clinical manifestations of HFMD, the clinical symptoms and pathological changes found in CA16 infected tree shrews still reveal a complete process of CA16 infection and strongly support the application of tree shrews as an animal model in CA16 infection research and vaccine evaluation.

References

- Arita M, Nagata N, Sata T, Miyamura T, Shimizu H. 2006. Quantitative analysis of poliomyelitis-like paralysis in mice induced by a poliovirus replicon. *The Journal of General Virology*, **87**(Pt 11): 3317-3327.
- Chang LY, Lin TY, Huang YC, Tsao KC, Shih SR, Kuo ML, Ning HC, Chung PW, Kang CM. 1999. Comparison of enterovirus 71 and coxsackievirus A16 clinical illnesses during the Taiwan enterovirus epidemic, 1998. *The Pediatric Infectious Disease Journal*, **18**(12): 1092-1096.
- Chen YJ, Meng FY, Mao QY, Li JX, Wang H, Liang ZL, Zhang YT, Gao F, Chen QH, Hu YM, Ge ZJ, Yao X, Guo HJ, Zhu FC, Li XL. 2014. Clinical evaluation for batch consistency of an inactivated enterovirus 71 vaccine in a large-scale phase 3 clinical trial. *Human Vaccines & Immunotherapeutics*, **10**(5): 1366-1372.
- Dong CH, Liu LD, Zhao HL, Wang JJ, Liao Y, Zhang XM, Na RX, Liang Y, Wang LC, Li QH. 2011. Immunoprotection elicited by an enterovirus type 71 experimental inactivated vaccine in mice and rhesus monkeys. *Vaccine*, **29**(37): 6269-6275.
- Fan Y, Huang ZY, Cao CC, Chen CS, Chen YX, Fan DD, He J, Hou HL, Hu L, Hu XT, Jiang XT, Lai R, Lang YS, Liang B, Liao SG, Mu D, Ma YY, Niu YY, Sun XQ, Xia JQ, Xiao J, Xiong ZQ, Xu L, Yang L, Zhang Y, Zhao W, Zhao XD, Zheng YT, Zhou JM, Zhu YB, Zhang GJ, Wang J, Yao YG. 2013. Genome of the Chinese tree shrew. *Nature Communications*, **4**: 1426.
- Goto K, Sanefuji M, Kusuhara K, Nishimura Y, Shimizu H, Kira R, Torisu H, Hara T. 2009. Rhombencephalitis and coxsackievirus A16. *Emerging Infectious Diseases*, **15**(10): 1689-1691.
- Han JB, Zhang GH, Duan Y, Ma JP, Zhang XH, Luo RH, Lü LB, Zheng YT. 2011. Sero-epidemiology of six viruses natural infection in *Tupaia belangeri chinensis*. *Zoological Research*, **32**(1): 11-16. (in Chinese)
- Hung HC, Chen TC, Fang MY, Yen KJ, Shih SR, Hsu JT, Tseng CP. 2010. Inhibition of enterovirus 71 replication and the viral 3D polymerase by aurintricarboxylic acid. *Journal of Antimicrobial Chemotherapy*, **65**(4): 676-683.
- Li RC, Liu LD, Mo ZJ, Wang XY, Xia JL, Liang ZL, Zhang Y, Li YP, Mao QY, Wang JJ, Jiang L, Dong CH, Che YC, Huang T, Jiang ZW,

- Xie ZP, Wang LC, Liao Y, Liang Y, Nong Y, Liu JS, Zhao HL, Na RX, Guo L, Pu J, Yang EX, Sun L, Cui PF, Shi HJ, Wang JZ, Li QH. 2014. An inactivated enterovirus 71 vaccine in healthy children. *The New England Journal of Medicine*, **370**(9): 829-837.
- Liu QW, Shi JP, Huang XL, Liu F, Cai YC, Lan K, Huang Z. 2014. A murine model of coxsackievirus A16 infection for anti-viral evaluation. *Antiviral Research*, **105**: 26-31.
- Lo SH, Huang YC, Huang CG, Tsao KC, Li WC, Hsieh YC, Chiu CH, Lin TY. 2011. Clinical and epidemiologic features of Coxsackievirus A6 infection in children in northern Taiwan between 2004 and 2009. *Journal of Microbiology, Immunology and Infection*, **44**(4): 252-257.
- Mao Q, Wang Y, Yao X, Bian L, Wu X, Xu M, Liang Z. 2013. Coxsackievirus A16: Epidemiology, diagnosis, and vaccine. *Human Vaccines & Immunotherapeutics*, **10**(2): 360-367.
- Mou J, Dawes M, Li Y, He Y, Ma H, Xie X, Griffiths S, Cheng J. 2014. Severe hand, foot and mouth disease in Shenzhen, South China: what matters most? *Epidemiology and Infection*, **142**(4): 776-788.
- Tan CW, Lai JK, Sam IC, Chan YF. 2014. Recent developments in antiviral agents against enterovirus 71 infection. *Journal of Biomedical Science*, **21**: 14.
- Ong KC, Badmanathan M, Devi S, Leong KL, Cardoso MJ, Wong KT. 2008. Pathologic characterization of a murine model of human enterovirus 71 encephalomyelitis. *Journal of Neuropathology and Experimental Neurology*, **67**(6): 532-542.
- Wang CY, Li LF, Wu MH, Lee CY, Huang LM. 2004a. Fatal coxsackievirus A16 infection. *The Pediatric Infectious Disease Journal*, **23**(3): 275-276.
- Wang YF, Chou CT, Lei HY, Liu CC, Wang SM, Yan JJ, Su IJ, Wang JR, Yeh TM, Chen SH, Yu CK. 2004b. A mouse-adapted enterovirus 71 strain causes neurological disease in mice after oral infection. *Journal of Virology*, **78**(15): 7916-7924.
- Wang YR, Sun LL, Xiao WL, Chen LY, Wang XF, Pan DM. 2013b. Epidemiology and clinical characteristics of hand foot, and mouth disease in a Shenzhen sentinel hospital from 2009 to 2011. *BMC Infectious Diseases*, **13**: 539.
- WHO. 1988. Procedure for Using the Lyophilized LBM Pools for Typing Enterovirus, Geneva.
- Xu L, Zhang Y, Liang B, Lü LB, Chen CS, Chen YB, Zhou JM, Yao YG. 2013. Tree shrews under the spot light: emerging model of human diseases. *Zoological Research*, **34**(2): 59-69.
- Yang E, Cheng C, Zhang Y, Wang J, Che Y, Pu J, Dong C, Liu L, He Z, Lu S, Zhao Y, Jiang L, Liao Y, Shao C, Li Q. 2014. Comparative study of the immunogenicity in mice and monkeys of an inactivated CA16 vaccine made from a human diploid cell line. *Human Vaccines & Immunotherapeutics*, **10**(5): 1266-1273.
- Yang MB, Li N, Li F, Zhu QQ, Liu X, Han QY, Wang YW, Chen YP, Zeng XY, Lv Y, Zhang PP, Yang CL, Liu ZW. 2013. Xanthohumol, a main prenylated chalcone from hops, reduces liver damage and modulates oxidative reaction and apoptosis in hepatitis C virus infected *Tupaia belangeri*. *International Immunopharmacology*, **16**(4): 466-474.
- Zhang XM, Zhao HL, Wang JJ, Liao Y, Na RX, Wang LC, Liu LD, Gao JH, Tang DH, Wang CZ, Li QH. 2011a. Evaluation of immune responses and related patho-inflammatory reactions of a candidate inactivated EV71 vaccine in neonatal monkeys. *National Medical Journal of China*, **91**(28): 1977-1981.
- Zhang Y, Cui W, Liu LD, Wang JJ, Zhao HL, Liao Y, Na RX, Dong CH, Wang LC, Xie ZP, Gao JH, Cui PF, Zhang XM, Li QH. 2011b. Pathogenesis study of enterovirus 71 infection in rhesus monkeys. *Laboratory Investigation*, **91**(9): 1337-1350.
- Zhang Y, Yang EX, Pu J, Liu LD, Che YC, Wang JJ, Liao Y, Wang LC, Ding D, Zhao T, Ma N, Song M, Wang X, Shen D, Tang DD, Huang HT, Zhang ZX, Chen D, Feng MF, Li QH. 2014. The gene expression profile of peripheral blood mononuclear cells from EV71-infected rhesus infants and the significance in viral pathogenesis. *PLoS One*, **9**(1): e83766.
- Zhu FC, Xu WB, Xia JL, Liang ZL, Liu Y, Zhang XF, Tan XJ, Wang L, Mao QY, Wu JY, Hu YM, Ji TJ, Song LF, Liang Q, Zhang BM, Gao Q, Li JX, Wang SY, Hu YS, Gu SR, Zhang JH, Yao GH, Gu JX, Wang XS, Zhou YC, Chen CB, Zhang ML, Cao MQ, Wang JZ, Wang H, Wang N. 2014. Efficacy, safety, and immunogenicity of an enterovirus 71 vaccine in China. *The New England Journal of Medicine*, **370**(9): 818-828.